Materials Physics and Mechanics 48 (2022) 136-146
Research article

Received: March 3, 2022
Accepted: March 22, 2022

THE INTERMETALLIC COMPOUNDS FORMATION AND MECHANICAL PROPERTIES OF COMPOSITES IN THE NI-AL SYSTEM

O.Y. Kurapova[1]✉, I.V. Smirnov[1], E.N. Solovyeva[2], Y.V. Konakov[3], T.E. Lomakina[1], A.G. Glukharev[1], V.G. Konakov[3]

[1]St. Petersburg State University, St. Petersburg, Russia

[2]Peter the Great St. Petersburg Polytechnic University, St. Petersburg, Russia

[3]Institute for Problems of Mechanical Engineering RAS, St. Petersburg, Russia

✉ plyshka@gmail.com

Abstract. Aluminum-nickel (Al-Ni) based intermetallic compounds are regarded as the promising materials for the high-temperature engineering applications, including harsh environments. So far, a satisfactory modeling has been done to analyze the structural properties, heats of formation, elastic properties and electronic energy band structures of Al-Ni intermetallic compounds. However, the experimental studies on Al-Ni intermetallic compounds formation and the data on the structure and mechanical properties are fragmentary in the literature. In the present work, the intermetallic compounds in Al-Ni system were obtained from nanonickel powder and micron-sized aluminum powders for the first time using modified powder metallurgy technique. Phase formation and structures of powders and consolidated materials were investigated via XRD, SEM, EDX and hydrostatic weighting. Via XRD it was shown, that despite the strong interactions between Ni and Al the formation of intermetallic compounds in the system is hindered. The density of consolidated specimens increases with nickel content increase. The sample 10nNi with the highest content of Al3Ni showed the best mechanical properties among the other specimens: Due to the reinforcement effect of the intermetallic compound, the sample with the highest content of Al3Ni showed the microhardness of 161±39 HV.

Keywords: intermetallic compound, nickel aluminide, phase formation, tensile strength, hardness, powder metallurgy technique

Acknowledgements*. This work was supported by Russian foundation for basic research (RSBF #18-29-19086). SEM and EDX data of the powders and consolidated specimens were obtained at the Research park of St. Petersburg State University «Center for Geo-Environmental Research and Modeling (GEOMODEL)» and «Interdisciplinary Center for Nanotechnology» respectively.*

Citation: Kurapova O.Y., Smirnov I.V., Solovyeva E.N., Konakov Y.V, Lomakina T.E., Glukharev A.G., Konakov V.G. The intermetallic compounds formation and mechanical properties of composites in the Ni-Al system // Materials Physics and Mechanics. 2022, V. 48. N. 1. P. 136-146. DOI: 10.18149/MPM.4812022_12.

http://dx.doi.org/10.18149/MPM.4812022_12

1. Introduction

Due to the high melting point, relatively low density and great corrosion resistance, transition metals aluminides have attracted a prominent attention as the candidates for high-temperature applications in the harsh environments as aircraft engines, high-temperature edges on aircraft wings and rocket fins, automobile engine valves, turbochargers [1,2]. Besides, unique chemical and physical properties of the intermetallic compounds make them promising materials to promote the electrocatalytic reactions [3-5]. This group of structural materials exhibit intermediate properties between ceramics and metals. A number of highly ordered intermetallic compounds stable up to melting point are formed in the Al-Fe [6-8], Al-Co [2,9,10], Al-Ru [11] and Al-Ni [1,12] and multicomponent systems [13-15]. Among them, Al-Ni system should be highlighted. According to the updated phase diagram data [16], five nickel aluminides are formed in the Al-Ni system, namely, Al_3Ni (orthorombic), Al_3Ni_2 (trigonal), AlNi (bcc), Al_3Ni_5 (orthorombic) and $AlNi_3$ (fcc). The thermodynamic data of the compounds were investigated thoroughly both experimentally and using first-principle calculations [1,12,17]. In all cases the enthalpies of formation at 298 K exhibit the pronounced minimum at the Ni:Al ratio 50:50 equal to NiAl compound. The enthalpies of formation obtained by solution and direct reaction calorimetry are -63.5 kJ/mol of atoms for Al_3Ni_2, 301 K; for AlNi -66.1 kJ/mol of atoms, 298 K, and for $AlNi_3$ -41.3 kJ/mol of atom [17,18]. Based on the data on the enthalpies of formation and dissolution, excess of entropies of formation, free Gibbs energies, it was concluded that the advanced aluminides are $AlNi_3$ and AlNi. They show the strongest chemical interaction between Ni and Al, remain ordered up to melting points, and thus are the potential candidates for practical applications. So in the recent decades for the two compounds equilibrium lattice constants, the elastic constants, the cohesive energies, and the effective defect formation energies have been studied in detail. As it is mentioned by Zamazande in the great review (7) like ceramics, all intermetallics suffer from their low ductility, particularly at low and intermediate temperatures. Recently, the structural properties, heats of formation, elastic properties and electronic energy band structures of Al–Ni intermetallic compounds have been analyzed systematically using density functional theory (DFT) and the plane-wave pseudopotential technique implemented in the CASTEP package (1). According to authors, all the Al–Ni intermetallic compounds are mechanically stable. Based on the calculated ratio of shear modulus to bulk modulus, it was concluded that AlNi, Al_3Ni, AlNi and Al_3Ni_5 compounds are ductile materials, whereas Al_4Ni_3 and Al_3Ni_2 are brittle materials. However, most of the data on phase formation, hardness and mechanical properties in the intermetallic compounds of Ni-Al system were obtained via the computational approach. The experimental data in this field is very limited and not systematic [19-21] Thus, the aim of the present research is to fill this gap and investigate the phase formation, tensile properties and hardness of the intermerallics and intermediate composites in Ni-Al system.

2. Methods

Nanosized nickel powder (nNi, purity ≥ 99.76%, average particle powder size 70 nm, "Advanced Powder Technologies", Ltd., Russia) and micron-sized aluminum powder (Al, particle powder size no more than 40 μm, purity ≥ 98.2%, "Advanced Powder Technologies", Ltd., Russia) were used as a starting material for the metal materials manufacturing. Powder mixtures containing 10-80 mol.% nNi were prepared according to phase diagram data [22] in order to obtain intermetallic compounds as well composites, containing intermetallic compounds. The specimens were fabricated using the modified powder metallurgy technique, suggested in the previous publications of authors, for nickel and aluminum based composites [23-25]. For that, powder mixtures of different compositions were grinded in a planetary mill (Pulverisete-6 planetary mill, 350 rpm for 3.5 hours with 2 minutes reverse cycles). Since nNi

powder is highly reactive, the milling was performed in the atmosphere of nitrogen. The obtained powders were compacted using cold pressing technique (uniaxial pressure, 12.5 ton, 15 min). The pellets with 25 mm diameter and 9 mm height were manufactured. Then the specimens were annealed in a vacuum furnace at 600°C for 1 hour and were left to cool down to room temperature within the furnace. The composition of fabricated specimens is listed in Table 1.

Table 1. The numeration of specimens

Specimen	5nNi	10nNi	16nNi	23nNi	31nNi	40nNi	51nNi	64nNi	80nNi
Composition, mol.%	95Al-5nNi	90Al-10nNi	84Al-16nNi	77Al-23nNi	69Al-31nNi	60Al-40nNi	49Al-51nNi	36Al-64nNi	20Al-80nNi

The identification of the phase composition of the specimens was performed by X-ray diffraction analysis (XRD, SHIMADZU XRD-6000, Cu-Kα at α=1.5406 Å). Scanning electron microscopy (SEM, Hitachi S-3400N) and high resolution scanning electron microscopy (HR-SEM, Zeiss Merlin) were used to analyze the microstructures of powder mixtures after milling and fabricated specimens. Apparent density of fabricated specimens was measured by hydrostatic weighting technique (scales RADWAG 220 c/xc, Poland). Each sample was weighted in air and then in isopropyl alcohol. Mechanical tests were carried out via uniaxial tension using SHIMADZU AG-50kNX test machine at the strain rate of 10^{-3} s^{-1}. The dog-bone shaped samples were cut along the cross-section of the pellets using an electrical erosion machine. The size of working part of samples was 6 mm in length, 2 mm in width and 1.2 mm in thickness. The data was averaged over 3 samples per each specimen. Vickers microhardness tests (Shimadzu HMV-G21DT) were performed using diamond pyramidal indenter with 2 kN load applied for 15 seconds. Microhardness value was averaged over 15 tests along the specimen's cross-section.

3. Results and Discussion

The phase composition and microstructure of the powder mixture after milling. In order to estimate the intermetallic formation during the milling in a planetary mill, the 40nNi powder was investigated via XRD. The XRD pattern of the specimen after milling is presented in Fig. 1.

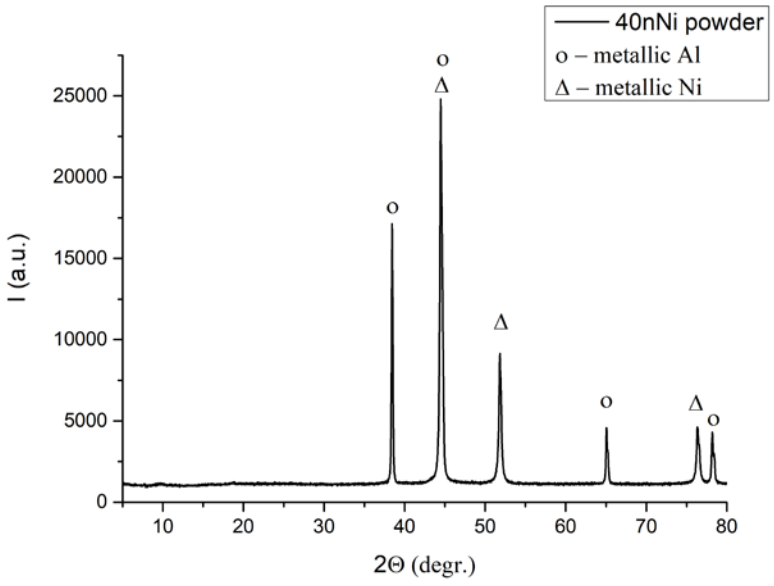

Fig. 1. XRD pattern of the 16nNi specimen after milling for 3.5 hours

As it is seen from XRD pattern (Fig. 1) , the specimen consists of two phases, i.e. metallic aluminum and nickel. The peaks, corresponding to Ni are present in the XRD pattern at 2Θ=44.3, 41.7, 76.3° and those to Al are at 2Θ=38.4, 44.8, 78.3° (marked by triangles and circles in Fig. 1). No other peaks corresponding to oxides or intermetallic compounds are seen. Indeed, the residual amounts of oxygen present in the gaseous nitrogen are not enough to initiate intensive nNi and Al powders oxidation, resulting in the oxides' formation. At the same time, such high energy milling is not enough for the *in situ* formation of the intermetallic compounds during milling. Closer examination of powders microstructure before and after milling was performed using HR SEM (see, Fig. 2).

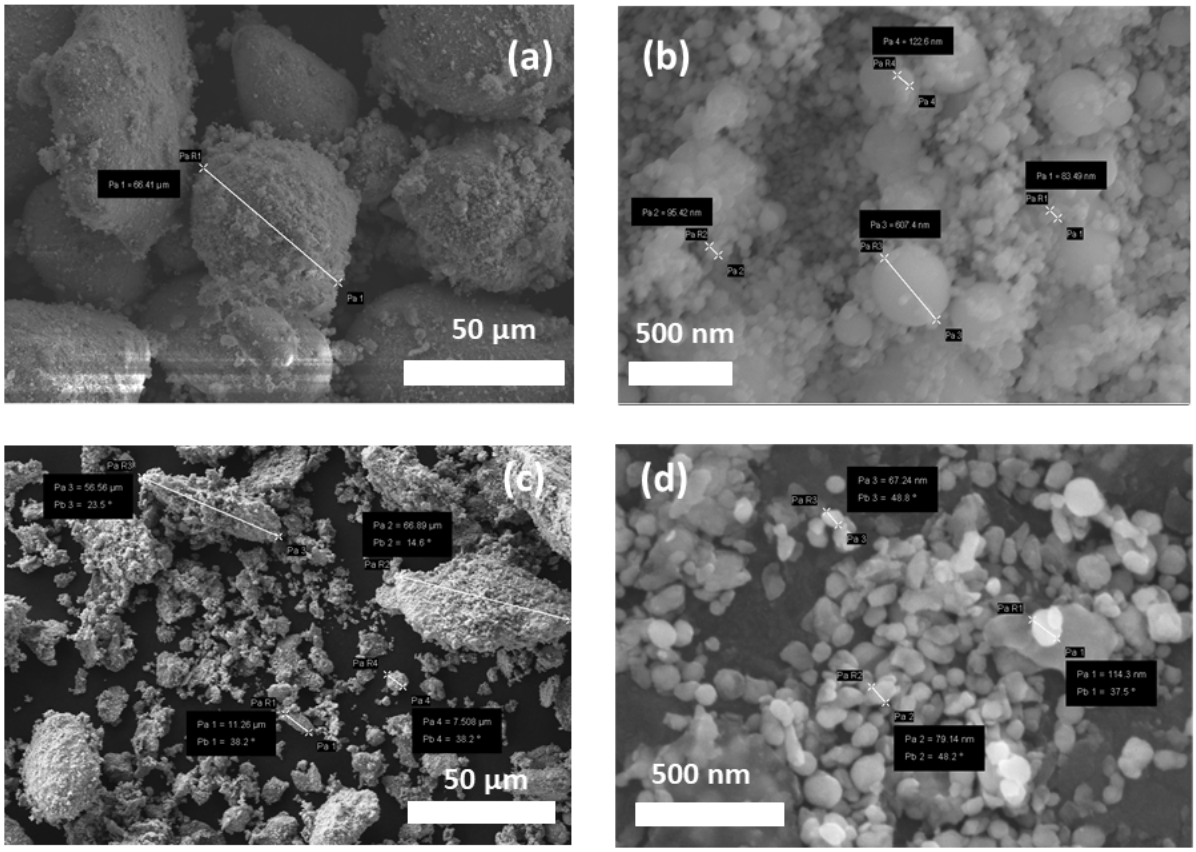

Fig. 2. (a) The 40nNi powder before milling, magnification ×1000; (b) The nickel nanoparticles in 40nNi powder before milling, magnification, ×50000; (c) The 16nNi powder after milling, magnification ×1000; (d) nNi particles on the surface of Al particle, magnification ×100 000

Figure 2a shows the structure of as-prepared 40nNi powder. The initial powder consists of the nearly spherical Al particles with typical sizes of ~65 µm. Coarse Al particles are irregularly covered by smaller agglomerates. At the higher magnification, it is seen that agglomerates consist of spherical nanosized Ni powder with particle sizes ~80-120 nm (see, Fig. 2b). It corresponds to the mean size indicated by the producer. The individual Ni particles have sizes up to 600 nm, but their amount is negligible. Milling at 450 rpm during 3.5 hours results in significant Al powder refinement. Typical sizes of the obtained agglomerates can be estimated as being 7-15 µm. Their particle shape change to lamellar flake-like geometry, which is, likely, due to high ductility of metallic aluminum. The surfaces of Al particles are homogeneously covered by nNi particles after milling. Milling affects nNi particles as well, resulting in their flattening without significant mean size change. Similar results were obtained for the other compositions studied. Thus, it can be concluded that chosen milling

conditions result in the effective homogenization of the powder mixture and some particle size decrease. This decrease results in specific surface area increase for the contacting powders and should favor intermetallic phases formation.

The structure of the consolidated specimens. The phase composition of the consolidated specimens is shown in Fig. 3 and summarized in Table 2.

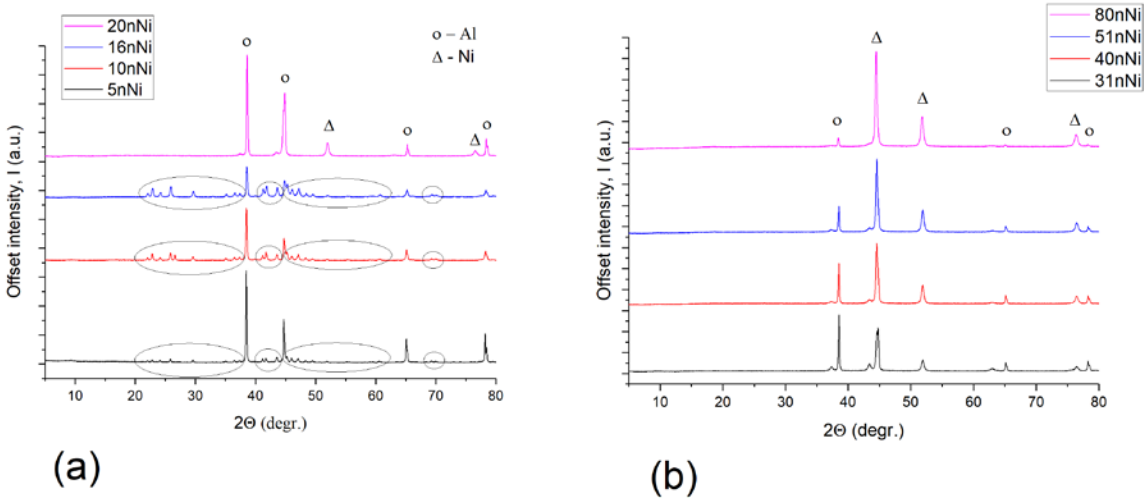

Fig. 3. XRD data obtained for the specimens of Al-Ni system: a – 5nNi, 10nNi, 16nNi, 20nNi; b – 31nNi, 40nNi, 51nNi, 80nNi. The circles stand for metallic Al, the triangles are for metallic Ni. The groups of peaks in the circles are referred to Al_3Ni

Table 2. Phase composition of Specimens according to XRD data, relative density and hardness of Specimens

Specimens	Phase composition	Relative density, %	Hardness, Hv
5nNi (90Al-10Ni)	Al+Al_3Ni	81.60+1.15	35±4
10nNi (80Al-20Ni)	Al+Al_3Ni	75.46+0.03	77±11
16nNi (70Al-30Ni)	Al+Al_3Ni	60.27+0.05	161±39
23nNi (60Al - 40Ni)	Al+Ni	66.90+0.78	35±3
31nNi (50Al - 50Ni)	Al+Ni	64.80+0.84	50±9
40nNi (40Al - 60Ni)	Al+Ni	68.75+1.11	-
51nNi (30Al - 70Ni)	Al+Ni	64.63+1.62	-
64nNi (20Al - 80Ni)	Al+Ni	66.21+1.84	83±11
80nNi (10Al - 90Ni)	Al+Ni	71.16+1.15	77±16

As it follows from XRD patterns, the specimens consist of at least two phases. Despite mentioned strong interaction between Ni and Al and preliminary mechanical activation of powder mixtures, the formation of the significant amounts of Al_3Ni takes place only in 5nNi, 10nNi and 16nNi specimens (see groups of reflections marked by the circles). Specimen with

16nNi demonstrates highest Al_3Ni content near 30 wt.% (see Table 2). Further increase in the nickel content results in the binary phased specimens consisting of metallic Al and Ni. As it is seen from Table 2, phase composition of specimens with 64-80 mol.% nNi correspond to two metallic phases of nickel and aluminum.

Since the resolution limit of XRD technique does not exceed 3-5 wt.%, SEM and EDX analyses were made to track possible intermetallic compounds formation based on the microstructure and chemical composition of the specimens. The SEM photos are presented in Figs. 4 and 5.

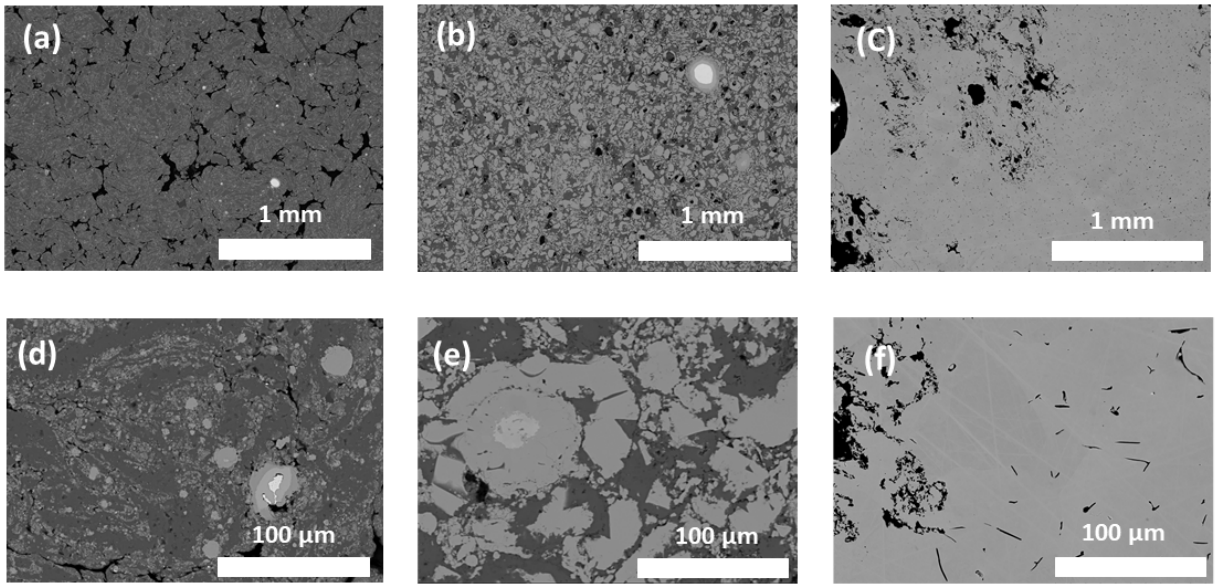

Fig. 4. SEM images of specimens (a), (d) – 10nNi; (b), (e) – 16nNi; (c), (f) – 23nNi under different resolution

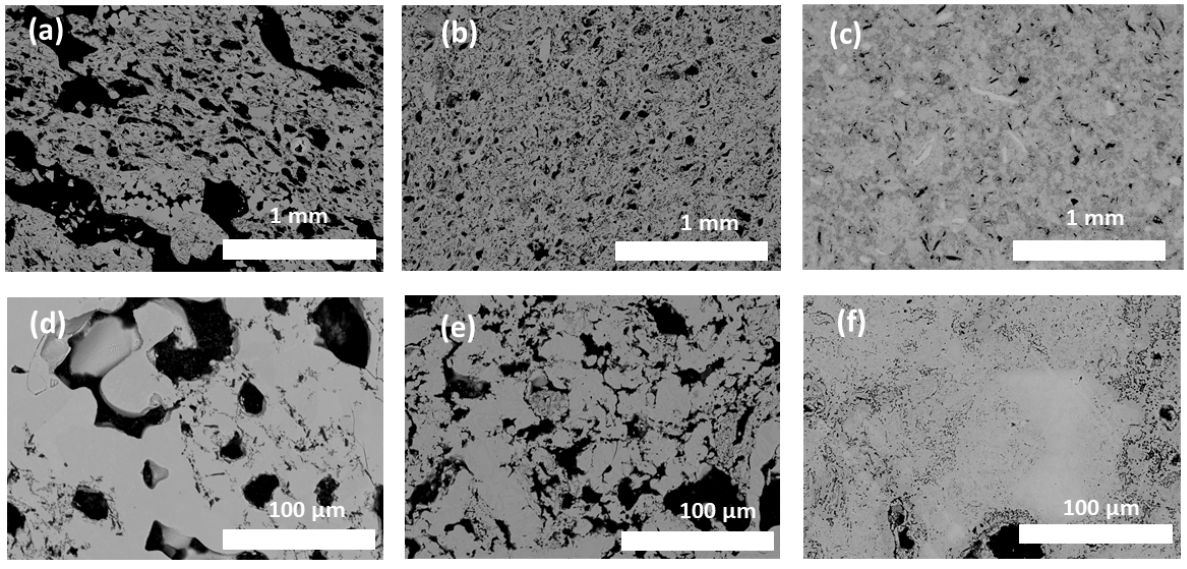

Fig. 5. SEM images of specimens (a), (d) – 31nNi; (b), (e) – 40nNi; (c), (f) – 80nNi under different resolution

As seen from Figs. 4(a) and (b), all specimens are significantly porous, being in accordance with the density measurements results (see Table 2). Specimens 5nNi and 10nNi exhibit similar structures, composed of coarse aluminium grains, separated by nickel phase

located along the grain boundaries. Specimen 5nNi has macroscopic elongated pores, whereas the pores in the 10nNi specimen are close to spherical. Both specimens contain bright zones, related to Al_3Ni intermetallic compound. At the higher magnification, in Figs. 4 (d) and (e) it is seen that these zones are mainly spherical surrounded by one more spherical diffusion zone formed during the solid-solid reaction between aluminium and nickel. The increase in nickel content to 80 mol. % induces the change of the specimen's structures and appearance of the large irregular pores randomly distributed. Generally, the size of pores decreases with nickel content and their distribution becomes homogeneous. The specimen with 80 mol.% Ni of exhibits the smallest pores size among the other specimens with the high Ni content (51-80nNi). Whole surface of the sample is covered by the pores network with sizes of the 5-10 μm despite the relative density of the specimen is high, i.e. 71.16%. Figure 6 illustrates the apparent density change with the Ni content increase in specimens together with the theoretical density.

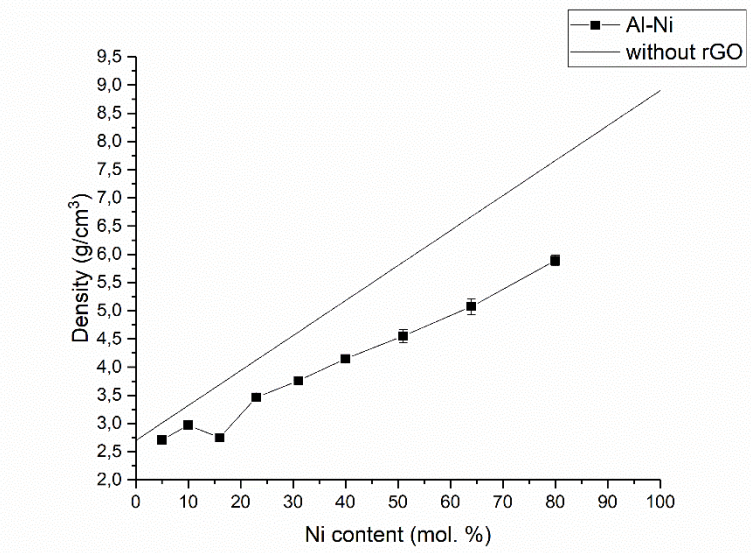

Fig. 6. The dependence of the apparent density on the Ni content in Ni-Al Specimens and the theoretical density calculated using mixture rule

As it is seen, the apparent density dependence of the nickel content is almost linear (Fig. 6). The exception is 16nNi composition, which is, likely, due to the highest Al_3Ni content. At the same time, 16nNi and 10nNi specimens show the smallest standard deviation. It should be noted that the theoretical density was calculated using mixture rules for Ni and Al. The formation of intermetallic compounds was not taken into account. The relative density of the specimens lies in a range 60.27 to 81.6% and is in the accordance with SEM results on high porosity of the samples. The lean structure and bi-phased composition of the specimens obtained resulted in their fragility. Thus, for mechanical tests it was possible to cut only three specimens: 5nNi, 10nNi and 80nNi, that showed relative density over 70%. Stress-strain diagram obtained for the specimens is shown in Fig. 7.

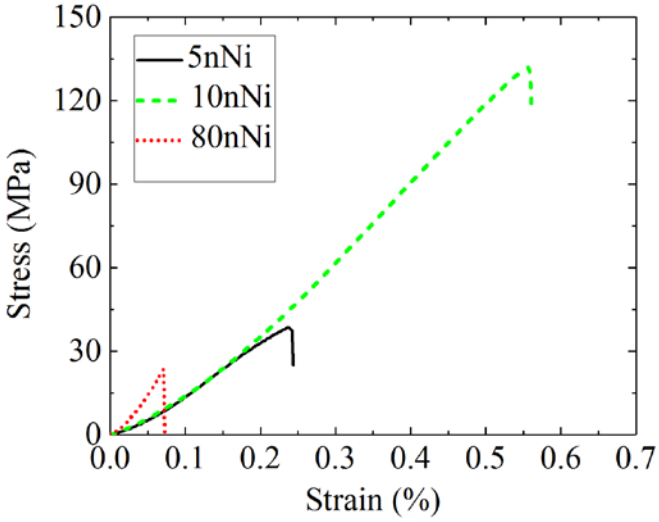

Fig. 7. The stress-strain diagram obtained for 5nNi, 10nNi and 80nNi

The fracture of the specimens took place during the stage of the elastic deformation. The 10nNi specimen showed the highest tensile strength and elongation, being σ_c = 132±0.3 MPa and ε_c=0.53±0.04%. Despite close chemical composition, 5nNi showed the significantly lower tensile strength (42±4 MPa). That may be due to the difference in phase composition, indeed, 10nNi specimen has higher content of Al_3Ni intermetallic compound. The 80nNi specimen demonstrated drastically reduced tensile strength compared to other specimens investigated and the data for pure bulk Al and nNi specimens [26,27]. On the other hand, the microhardness tests revealed several additional features of the Al-Ni system. The 16nNi specimen exhibited maximum HV value, 161±39 HV. However, high porosity of the consolidated samples did not allow preparing the samples of the correct shape for the tensile tests. Despite the significantly different tensile strength, 10nNi and 80nNi specimens showed similar microhardness values.

Table 3. The results of the mechanical tests ε_c – maximum elongation, σ_c – ultimate tensile strength (UTS), E – Young's modulus.

Specimen	ε_c, %	UTS σ_c, MPa	E, GPa
80nNi	0.09±0.02	22±3	26.6±9.3
10nNi	0.53±0.04	132±0.3	24.9±1.9
5nNi	0.27±0.08	42±4	15.9±3.1

In summary, one can see that the use of the modified powder metallurgy approach allows fabricating the composite specimens containing Al and Al_3Ni intermetallic compound. The obtained data is in accordance with the data of [28] where the similar composition was obtained by alloying 5wt%Ni and Al powders. The UTS value of 10nNi specimen with the highest Al_3Ni content is slightly higher than the one for the coarse sample obtained in [28] from the melt (132 MPa and 110 MPa, respectively). Considering obtained microhardness data and literature [28-31] it can be concluded that the Al_3Ni particles act as reinforcements of the ductile Al matrix in the Al-rich region. Despite the literature data on the calculated thermodynamic properties and high interaction ratio between Al and Ni [1], no AlNi or Al_3Ni_2 compounds were detected in the investigated samples. Both metallic Al and Ni have body centered crystal (bcc) structures. In turn, the structures of Al_3Ni_2 (trigonal) and Al_3Ni_5 (orthorhombic) differ a lot from the initial reagents. Thus, it can be suggested that the formation of Al_3Ni_2 and Al_3Ni_5 in Al-Ni system during the sintering is, most likely, hindered

by the necessity of the crystal structure reorganization. The AlNi in turn has the same bcc structure and $AlNi_3$ has close cubic but a face centered crystal structures. The formation of the compound does not require significant structural changes. However, it is, likely, governed by the slow diffusion in solid.

4. Conclusion

Via SEM and XRD data it was shown that the milling of Ni and Al powders mixture results in the significant grain refinement, homogenization of the mixture and is not accompanied by the intermetallic compounds' formation. Using XRD data, it was demonstrated that the significant amounts of Al_3Ni with Al phase admixture are formed at the Ni content up to 16 mol.%. SEM, EDX and density measurement data showed that the complex phase composition of samples results in the loose porous structure of specimens with the relative density from 60.27 to 81.6%. Mechanical tests revealed that the 10nNi specimen showed the highest tensile strength and elongation, being σ_c = 132±0.3 MPa and ε_c=0.53±0.04%.

References

[1] Shi D, Wen B, Melnik R, Yao S, Li T. First-principles studies of Al-Ni intermetallic compounds. *J. Solid State Chem*. 2009;182(10): 2664-2669.
[2] Hadef F. Synthesis and disordering of B2 TM-Al (TM = Fe, Ni, Co) intermetallic alloys by high energy ball milling: A review. *Powder Technol*. 2017;311: 556-578.
[3] Rößner L, Armbrüster M. Electrochemical Energy Conversion on Intermetallic Compounds: A Review. *ACS Catal*. 2019;9(3): 2018-2062.
[4] Wang Y, Hall AS. Room-Temperature Synthesis of Intermetallic Cu–Zn by an Electrochemically Induced Phase Transformation. *Chem. Mater*. 2021;33(18): 7309-7314.
[5] Rößner L, Schwarz H, Veremchuk I, Zerdoumi R, Seyller T, Armbrüster M. Challenging the Durability of Intermetallic Mo–Ni Compounds in the Hydrogen Evolution Reaction. *ACS Appl. Mater. Interfaces*. 2021;13(20): 23616-2326.
[6] Gąsior W, Dębski A, Moser Z. Formation enthalpy of intermetallic phases from Al–Fe system measured with solution calorimetric method. *Intermetallics*. 2012;24: 99-105.
[7] Zamanzade M, Barnoush A, Motz C. A Review on the Properties of Iron Aluminide Intermetallics. *Crystals*. 2016;6(1): 10.
[8] Canakcı A, Ozkaya S, Erdemir F, Karabacak AH, Celebi M. Effects of Fe–Al intermetallic compounds on the wear and corrosion performances of AA2024/316L SS metal/metal composites. *J. Alloys Compd*. 2020;845: 156236.
[9] Stein F, He C, Dupin N. Melting behaviour and homogeneity range of B2 CoAl and updated thermodynamic description of the Al–Co system. *Intermetallics*. 2013;39: 58-68.
[10] Ilyushin GD. Symmetry and Topology Code of the Cluster Self-Assembly of Intermetallic Compounds A 2 [16] B 4 [12] of the Friauf Families Mg2Cu4 and Mg2Zn4. *Crystallogr. Reports*. 2018;63(4): 543-552.
[11] Klein T, Pauly C, Mücklich F, Kickelbick G. Al and Ru nanoparticles as precursors for Ru–Al intermetallics. *Intermetallics*. 2020;124: 106851.
[12] Pretorius R, de Reus R, Vredenberg AM, Saris FW. Use of the effective heat of formation rule for predicting phase formation sequence in AlNi systems. *Mater Lett*. 1990;9(12): 494-499.
[13] Gholizadeh R, Shabestari SG. Investigation of the Effects of Ni, Fe, and Mn on the Formation of Complex Intermetallic Compounds in Al-Si-Cu-Mg-Ni Alloys. *Metall. Mater. Trans. A*. 2011;42(11): 3447-58.
[14] Kim JT, Hong SH, Park JM, Eckert J, Kim KB. Microstructure and mechanical properties of hierarchical multi-phase composites based on Al-Ni-type intermetallic compounds in the Al-Ni-Cu-Si alloy system. *J. Alloys Compd*. 2018;749: 205-210.

[15] Somidin F, Maeno H, Toriyama T, McDonald SD, Yang W, Matsumura S, Nogita K. Direct observation of the Ni stabilising effect in interfacial (Cu,Ni)6Sn5 intermetallic compounds. *Materialia*. 2020;9: 100530.
[16] Okamoto H. Al-Ni (aluminum-nickel). *J. Phase Equilibria Diffus*. 2004;25(4): 394-394.
[17] Rzyman K, Moser Z. Calorimetric studies of the enthalpies of formation of Al3Ni2, AlNi and AlNi3. *Prog. Mater. Sci*. 2004;49(3–4): 581-606.
[18] Rzyman K, Moser Z, Watson RE, Weinert M. Enthalpies of formation of Ni3Al: Experiment versus theory. *J. Phase Equilibria*. 1996;17(3): 173-178.
[19] Jiang H, Ye S, Ma R, Yu P. Influences of sintering parameters on shape-retention ability of porous Ni3Al intermetallic fabricated by powder metallurgy. *Intermetallics*. 2019;105: 48-55.
[20] Liang W, Jiang Y, Hongxing D, He Y, Xu N, Zou J, Huang B, Liud CT. The corrosion behavior of porous Ni3Al intermetallic materials in strong alkali solution. *Intermetallics*. 2011;19(11): 1759-1765.
[21] Cui H, Wei N, Zeng L, Wang X, Tang H. Microstructure and formation mechanism of Ni-Al intermetallic compounds fabricated by reaction synthesis. *Trans. Nonferrous Met. Soc. China*. 2013;23(6): 1639-1645.
[22] Hilpert K, Kobertz D, Venugopal V, Miller M, Gerads H, Bremer FJ, Nickel H. Phase Diagram Studies on the Al- Ni System. *Zeitschrift für Naturforsch A*. 1987;42(11): 1327-1332.
[23] Konakov VG, Ovid'ko IA, Borisova N V., Solovyeva EN, Golubev SN, Kurapova OY, Novik NN, Archakov IY. Synthesis of the precursor for aluminum-graphene composite. *Rev. Adv. Mater. Sci*. 2014;39(1): 41-47.
[24] Konakov VG, Kurapova OY, Archakov IY. Improvement of Copper–Graphene Composites Properties due to the Lubricating Effect of Graphene in the Powder Metallurgy Fabrication Process. *Met. Mater. Int*. 2020;26(12): 1899-1907.
[25] Kurapova OY, Lomakin IV, Sergeev SN, Solovyeva EN, Zhilyaev AP, Archakov IY, Konakov VG. Fabrication of nickel-graphene composites with superior hardness. *J. Alloys Compd*. 2020;835: 155463.
[26] Kurapova O, Smirnov I, Solovyeva E, Archakov I, Konakov V. The effect of reduced graphene oxide (rGO) and thermally exfoliated graphite (TEFG) on the mechanical properties of "nickel-graphene" composites. *Lett Mater*. 2020;10(2): 164-169.
[27] Shao P, Yang W, Zhang Q, Meng Q, Tan X, Xiu Z, Qiao J, Yu Z, Wu G.Microstructure and tensile properties of 5083 Al matrix composites reinforced with graphene oxide and graphene nanoplates prepared by pressure infiltration method. *Compos. Part A Appl. Sci. Manuf*. 2018;109: 151-162.
[28] Osório WR, Peixoto LC, Canté MV, Garcia A. Microstructure features affecting mechanical properties and corrosion behavior of a hypoeutectic Al–Ni alloy. *Mater Des*. 2010;31(9): 4485-4489.
[29] Wen J, Cui H, Wei N, Song X, Zhang G, Wang C, Song Q. Effect of phase composition and microstructure on the corrosion resistance of Ni-Al intermetallic compounds. *J. Alloys Compd*. 2017;695: 2424-2433.
[30] Russell AM. Ductility in Intermetallic Compounds. *Adv Eng Mater*. 2003;5(9): 629-639.
[31] Varin RA, Winnicka MB. Plasticity of structural intermetallic compounds. *Mater Sci Eng A*. 1991;137: 93-103.

THE AUTHORS

Kurapova O.Y.
e-mail: plyshka@gmail.com
ORCID: 0000-0002-7148-7755

Smirnov I.V.
e-mail: i.v.smirnov@spbu.ru
ORCID: 0000-0003-2406-5418

Solovyeva E.N.
e-mail: glasscer@yandex.ru
ORCID: 0000-0002-7148-7755

Konakov Y.V.
e-mail: for-rams@yandex.ru
ORCID: 0000-0003-3942-6212

Lomakina T.E.
e-mail: st056239@student.spbu.ru
ORCID: 0000-0002-7148-7755

Glukharev A.G.
e-mail: gluharev1@gmail.com
ORCID: 0000-0003-2474-6918

Konakov V.G.
e-mail: vgkonakov@yandex.ru
ORCID: 0000-0002-5332-2121